

Parity effect does not mean a superconductor free of quasiparticles

E. T. Mannila,^{1,*} V. F. Maisi,^{1,2} H. Q. Nguyen,^{3,4} C. M. Marcus,³ and J. P. Pekola¹

¹*QTF Centre of Excellence, Department of Applied Physics, Aalto University, FI-00076 Aalto, Finland*

²*Division of Solid State Physics and NanoLund, Lund University, 22100 Lund, Sweden*

³*Center for Quantum Devices and Station Q Copenhagen,*

Niels Bohr Institute, University of Copenhagen, Copenhagen, Denmark

⁴*Nano and Energy Center, Hanoi University of Science, VNU, 120401 Hanoi, Vietnam*

(Dated: November 10, 2019)

We show that a superconducting device can show a clear parity effect in the number of electrons even when there is, on average, a single nonequilibrium quasiparticle present, by monitoring in real time the charge state of a superconducting island connected to normal leads by tunnel junctions. The quasiparticles are created by Cooper pairs breaking on the island at a rate of a few kHz. We demonstrate that the pair breaking is caused by the backaction of the single-electron transistor used as a charge detector. With sufficiently low probing currents, our superconducting island is free of quasiparticles 97% of the time.

In a superconductor, ideally all conduction electrons form Cooper pairs. The minimum energy for an unpaired quasiparticle excitation is Δ , the superconducting gap, which leads to a free energy difference between states with an even and odd number of electrons in the absence of subgap states. The resulting parity effect is commonly observed in features periodic in $2e$, with e the electron charge, in the transport through an island or by measuring the average charge in an isolated box [1–4]. In thermal equilibrium, the parity effect disappears at temperatures where quasiparticles are excited, around 200 mK for typical micron-scale aluminum structures, as the free energy difference disappears. A clean $2e$ periodicity of Coulomb blockade is often taken to suggest a device free of quasiparticles [5–8].

In addition to suppressing the parity effect [5, 9], quasiparticle excitations are generally detrimental for superconducting devices. In Josephson junction based qubits, quasiparticles tunneling across the junctions lead to decoherence [10, 11]. For quantum computing using Majorana zero modes in superconductor-semiconductor hybrids, topological protection is only present when the total fermion parity of the system stays constant, and the parity lifetime is a fundamental bound to the coherence time of such a qubit [12–14]. At low temperatures the quasiparticle density n_{qp} should be exponentially suppressed, and the parity lifetime consequently exponentially long. In practice, often a saturation of n_{qp} to values several orders of magnitude higher than that in thermal equilibrium is observed in experiments on superconducting qubits [10, 15, 16], resonators [17–19], and quantum capacitance [20] and kinetic inductance detectors [21]. Another quantity related to the quasiparticle density is the poisoning time or the time between successive quasiparticle tunneling events. Quasiparticle densities or poisoning times can be inferred from transport measurements [13, 14, 22–24] or qubit coherence times [25]. Even-to-odd transitions from quasiparticle tunneling can also be measured in real time with radio-frequency reflectom-

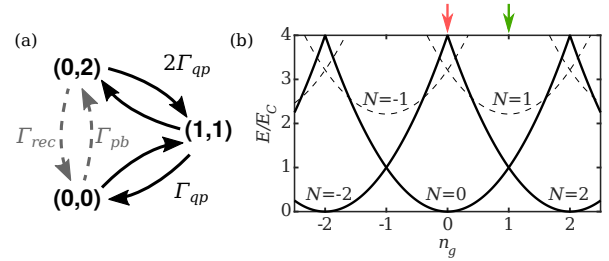


FIG. 1. (a) States (N, N_S) with N excess charges and N_S quasiparticle excitations on the superconducting island. Quasiparticle tunneling events occurring at rate Γ_{qp} are directly detected, while Cooper pairs break at a rate Γ_{pb} and recombine with Γ_{rec} . (b) The parity-dependent free energy $E = E_C(N - n_g)^2 + F(T_S) \times N \bmod 2$ of even (solid lines) and odd (dashed) charge states N , calculated at $k_B T_S / \Delta = 0.02$ and $E_C / \Delta = 0.33$. Red and green arrows show values of the gate offset n_g for the charge detector traces shown in Fig. 2.

etry [15, 26–28] or in the parity-dependent frequency shift of a transmon qubit [16, 29].

In this work we use a capacitively coupled charge detector to detect in real time parity and quasiparticles tunneling on and off a superconducting island. We observe parity-dependent tunneling rates arising from quasiparticle excitations allowing us to conclude that a single quasiparticle is residing on the island, even though the parity effect is still clearly visible. The measured occupation probabilities and tunneling rates are quantitatively explained with a simple model incorporating single-electron tunneling and quasiparticle recombination, with the nonequilibrium Cooper pair breaking rate on the island as the only free parameter. We further show that the Cooper pair breaking is caused by the backaction of the charge detector [9]. This is a critical issue for Majorana qubit proposals incorporating charge detectors as part of the qubit readout chain [30, 31].

We characterize the state of the superconducting island following Ref. [23], with the excess charge N and

number of excitations N_S on the island, where N and N_S are integers of the same parity. The relevant processes in our system are schematically shown in Fig. 1(a). If there are two or more excitations on the island, they can recombine to a Cooper pair with rates $\Gamma_{rec}(N_S)$. We include recombination via the electron-phonon coupling. Cooper pairs on the island can break, creating two excitations, with a rate Γ_{pb} assumed independent of the state of the island. Here Γ_{pb} is a residual rate present in addition to the electron-phonon pairbreaking rate, which is vanishingly small at the temperatures of the experiment. We directly detect the quasiparticle tunneling events between the superconducting island and normal metal leads at temperature T_N occurring at rates Γ_{qp} , which change both the charge and number of excitations by one. If excess quasiparticles are present (the superconductor temperature $T_S > T_N$) but $k_B T_N \ll \Delta$, Γ_{qp} depends, for a range of energy gains, only on the quasiparticle density $n_{qp} = \sqrt{2\pi} D(E_F) \sqrt{\Delta k_B T_S} e^{-\Delta/k_B T_S}$ or the number of excitations $N_S = n_{qp} V$ as [32]

$$\Gamma_{qp} = \frac{n_{qp}}{2e^2 R_T D(E_F)}. \quad (1)$$

Here, R_T is the tunnel resistance of the tunnel junction, k_B is the Boltzmann constant, and $D(E_F)$ is the normal density of states (including spin) at the Fermi level, for which we use $2.15 \times 10^{47} \text{ J}^{-1} \text{ m}^{-3}$ [17]. In particular, having a single quasiparticle in the island with volume $V = 550 \text{ nm} \times 2 \text{ } \mu\text{m} \times 50 \text{ nm}$ and $R_T = 15.6 \text{ M}\Omega$ corresponds to a tunneling rate $\Gamma_{qp} = 110 \text{ Hz}$.

If Γ_{pb} is zero in the model above, we recover the thermal equilibrium case. The free energies of the charge states N of a superconducting island are $E = E_C(N - n_g)^2 + F(T_S) \times N \bmod 2$, which includes, in addition to the contribution of the charging energy $E_C = e^2/2C_\Sigma$ with C_Σ the total capacitance of the island, the free energy cost $F(T_S) \approx \Delta - k_B T_S \ln(D(E_F)V\Delta)$ of an unpaired excitation [1, 3]. The approximation is valid when $k_B T_S \ll \Delta$. These free energies are sketched in Fig. 1(b) as a function of the gate offset $n_g = C_g V_g/e$, where V_g is the voltage applied to a gate electrode coupled via capacitance C_g . When $F(T_S) > E_C$, as in our device below 120 mK, the ground state has even parity, and we would expect to see only two-electron tunneling events around odd n_g . The states with odd N should become significantly occupied only above the temperature $T_0 = \Delta/(k_B \ln(VD(E_F)\Delta)) \approx 190 \text{ mK}$, where a single quasiparticle is thermally excited on the island and $F(T_0) \approx 0$.

Our device, shown in Fig. 2(a), consists of a single-electron transistor (SET) with an aluminum island connected to copper leads with aluminum oxide tunnel barriers a few nanometers thick. The capacitively coupled charge detector, located $10 \text{ } \mu\text{m}$ from the superconducting island, is another SET, but with a copper island and aluminum leads. The devices were fabricated with standard

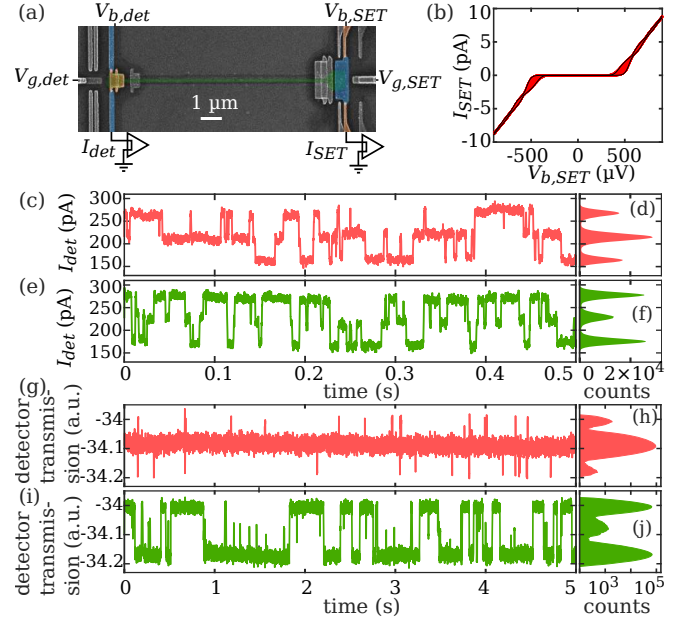


FIG. 2. (a) False color scanning electron micrograph of the device and measurement setup. The SET with a superconducting aluminum island (blue) connected to normal copper leads (orange) is shown on the right. The charge detector on the left side of the image is coupled to the island with a $10 \text{ } \mu\text{m}$ long chromium wire (green) under a 40 nm insulating aluminum oxide layer grown by atomic layer deposition. A gold ground plane (not shown) under the AlOx layer shunts the leads of the aluminum island. (b) Large-scale current-voltage characteristics of the superconducting island of sample A, measured (red) over several periods in the gate voltage $V_{g,SET}$ for each bias voltage $V_{b,SET}$. Black lines are simulations at gate offsets $n_g = 0$ and $n_g = 0.5$ with device parameters given in the text. (c,e) Real-time detector output of sample A at $V_{b,SET} = 0$ and $V_{b,det} = 490 \text{ } \mu\text{eV}$ with (c) $n_g = 0$ and (e) $n_g = 1$ after digital low pass filtering. Three charge states are occupied in both cases, but even charge states have a higher occupation probability. (d,f) Histograms of the traces shown in panels (c,e). (g,i) Real-time detector output of sample B at $V_{b,SET} = 0$ and $V_{b,det} = 350 \text{ } \mu\text{eV}$. (h,j) Histograms of the traces shown in panels (g,i). Note that in contrast to (d,f), a logarithmic scale is used here to show the minuscule occupation of the odd states.

electron-beam lithography and three-angle evaporation. We have measured two similar devices, samples A and B. Sample A was measured in a homemade plastic dilution refrigerator with a base temperature of 50 mK in a setup known to be well shielded against external microwave radiation [23, 32]. Sample B was measured in a dry dilution refrigerator with a base temperature of 20 mK in a setup with similar filtering and shielding solutions.

The energy gap $\Delta = 206 \text{ } \mu\text{eV}$ ($210 \text{ } \mu\text{eV}$), total tunnel resistance of the two junctions $70 \text{ M}\Omega$ ($40 \text{ M}\Omega$) and the charging energy $E_C = 0.33\Delta = 68 \text{ } \mu\text{eV}$ ($0.45\Delta = 95 \text{ } \mu\text{eV}$) of sample A (B) were determined by fitting the large-scale current-voltage characteristics as shown

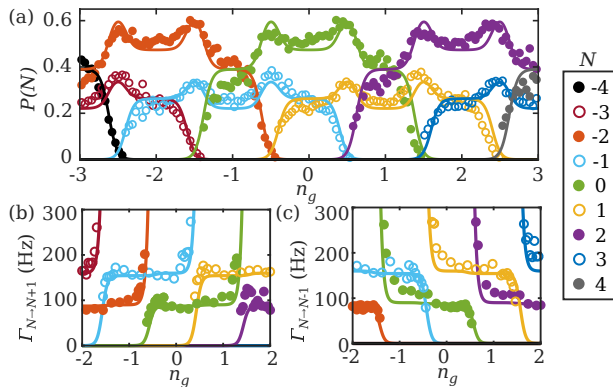


FIG. 3. (a) Occupation probabilities $P(N)$ and (b,c) tunneling rates $\Gamma_{N,N\pm 1}$ between charge states N over a range of gate offsets n_g in sample A. Filled (open) circles correspond to measured values for even (odd) N . There are always at least three charge states occupied with more than 10% probability, a nonequilibrium situation, but the most probable state always has even parity. The transition rates have plateaus at $\Gamma_{\text{even}} = 80$ Hz and $\Gamma_{\text{odd}} = 160$ Hz with the rate depending only on the parity of the initial state. These values correspond to a parity-dependent quasiparticle density on the island. Solid lines are numerical simulations with the Cooper pair breaking rate $\Gamma_{pb} = 4.6$ kHz as the only free parameter.

in Fig. 2(b). For the electron counting experiments, the superconducting island was kept at zero bias, and the island acts as a superconducting box connected to normal leads through the parallel resistance of the two junctions $R_T = 15.6$ M Ω (8.9 M Ω), with the junction sizes and resistances differing by a factor of 2 (2). The charge detectors were biased at a constant DC voltage $V_{b,det}$. For sample A, we record the amplified output current I_{det} . For sample B, we use the detector as a radio frequency SET [33] and monitor the transmitted power at 600 MHz through a lumped-element LC circuit in which the detector has been embedded [34, 35].

Figure 2(c-j) shows real-time traces of the charge detector output at $n_g = 0$ (c,d,g,h) and $n_g = 1$ (e,f,i,j). In sample A (Fig. 2(c-f)), three charge states are always occupied for a significant fraction of time, even though the charging energy ($E_C/k_B \approx 800$ mK) is much larger than the bath temperature of 60 mK. Most of the transitions are single-electron transitions. At $n_g = 0$ the state at $I_{det} = 200$ pA corresponding to $N = 0$ is more occupied than $N = \pm 1$ at 150 pA and 250 pA, while at $n_g = 1$ the state $N = 1$ at 220 pA has a lower occupation probability than $N = 0$ (170 pA) or $N = 2$ (270 pA). In sample B (Fig. 2(g-j)), where the setup allows using smaller detector currents, the odd states are occupied with almost two orders of magnitude lower probability, suggesting a much lower density of nonequilibrium quasiparticles.

We measure time traces across a range of n_g and extract the occupation probabilities of each charge state N , shown in Fig. 3(a). At all values of n_g there are three

or four charge states visible. This can be explained with a nonequilibrium quasiparticle population: intuitively, if there is a quasiparticle with energy $\Delta = 3E_C$ on the island, the energy cost of charging the island with one electron is possible to overcome. If $n_g = 0.5$, the charging part of the energy $E_C(N - n_g)^2$ is smaller than Δ for the states $N = -1, 0, 1$ and 2, which are the states that we observe. However, even in this nonequilibrium situation, the most probable state has always even parity as in thermal equilibrium.

The tunneling rates $\Gamma_{N \rightarrow M}$ of single-electron transitions, shown in Fig. 3(b-c), are determined from the time traces as the number of transitions from N to M divided by the total time spent in state N . In all of the transitions there is a range in n_g where the rate is approximately constant, as expected for quasiparticle tunneling. For the transitions with N even, the rate at the plateau is approximately $\Gamma_{\text{even}} = 80$ Hz, while for the odd-to-even transitions it is close to $\Gamma_{\text{odd}} = 160$ Hz. This confirms that the observed features are indeed caused by extra quasiparticles, but with a quasiparticle density that depends on the parity of the island. According to Eq. (1), the ratio $\Gamma_{\text{odd}}/\Gamma_{\text{even}}$ directly probes the ratio of the mean quasiparticle numbers $\langle N_S \rangle$ in even and odd charge states. Given that odd states contain at least one quasiparticle, the observed ratio $\Gamma_{\text{odd}}/\Gamma_{\text{even}} = \langle N_{S,\text{odd}} \rangle / \langle N_{S,\text{even}} \rangle \approx 2$ means that $\langle N_{S,\text{even}} \rangle \geq 0.5$ and at least two quasiparticles must be present for 25% of the time in even states as well.

To maintain such a quasiparticle population, quasiparticles must be generated either from Cooper pairs breaking or electrons tunneling from the leads with a total rate on the same order as with what they tunnel out or recombine. The expected recombination rate is 9.7 kHz for $N_S = 2$ and larger for more quasiparticles (assuming the electron-phonon coupling constant for aluminum $\Sigma = 1.8 \times 10^9$ W K $^{-5}$ m $^{-3}$ [23]), two orders of magnitude larger than the measured tunneling rates. A Cooper pair breaking rate much larger than the tunneling rates on the island itself is then needed to produce the observed excess quasiparticles, in contrast to models where quasiparticles tunnel in from the leads [5, 36]. Any broken Cooper pair on the island will, on average, recombine on the island itself before having time to tunnel out, and the quasiparticle population on the island is determined by the competition between pair breaking and recombination, with the tunnel contacts only serving to probe the resulting quasiparticle density.

We calculate numerically the transition rates between the different (N, N_S) states using the quasiparticle tunneling and recombination rates given in Ref. [23], and solve for the steady-state occupation probabilities. The solid lines in Fig. 3(a) are the occupation probabilities for each charge state with any number of excitations, while the solid lines in Figs. 3(b-c) are the average rates between different charge states. To reproduce

the significant occupation probabilities of the odd charge states, we need to include a Cooper pair breaking rate $\Gamma_{pb} = 4.6$ kHz. We are able to reproduce quantitatively all the features in the transition rates and occupation probabilities with only Γ_{pb} as a free parameter in our model. Other parameters are either determined from independent measurements (R_T , Δ , E_C) or they are known literature values (Σ , $D(E_F)$).

Some of the transitions interpreted as two successive single-electron events might be two-electron Andreev events (such as at 0.12 s in Fig. 2(e)), which are not included in the model. Yet their influence to obtained results is weak: assuming successive transitions from N to $N \pm 2$ occurring within 1 ms to be Andreev events decreases the inferred single-electron tunnel rates only by a few percent. The finite bandwidth of the detector (a few kHz) mostly causes the measured rates to underestimate the true rates at the quasiparticle-induced plateaus by 10% to 20% [37] and does not affect our main conclusions. In Fig. 3, we have corrected the simulated rates to account for finite bandwidth using the model of Ref. [37].

The time-averaged number of excitations from the simulations is $\langle N_S \rangle = 0.86$ in even charge states, 1.6 in odd states, and altogether 1.1. The equilibrium temperature where the parity effect is expected to disappear corresponds to a single quasiparticle being thermally excited. It is somewhat against the common view that the parity effect is clearly visible even with a single nonequilibrium excitation present, as we demonstrate here. The ratio of the pair breaking and recombination rates Γ_{pb}/Γ_{rec} determines the quasiparticle density. However, we cannot determine these two rates independently: the agreement between simulations and experiment in Fig. 3 remains equally good if Γ_{pb} and the electron-phonon coupling constant Σ setting Γ_{rec} are scaled up or down but by the same factor. The observed tunneling rates out of even charge states Γ_{even} do set a rough lower bound for Γ_{pb} : the tunneling rates $(N, 0)$ to $(N + 1, 1)$ for even N are vanishingly small around $n_g = N$. Any tunneling event means that two or more quasiparticles were already present in the even N state, which need to be created by pair breaking.

We now turn to the origin of the Cooper pair breaking rate observed. We repeat the measurement of time traces versus n_g in sample A at different detector bias voltages $V_{b,det}$ between 385 μ V and 560 μ V and extract the tunneling rates Γ_{even} and Γ_{odd} at the quasiparticle-induced plateaus. These are shown as a function of the detector current in Fig. 4. The tunneling rates out of both even and odd states increase linearly with detector current, but Γ_{even} extrapolates to zero at $I_{det} = 0$, while Γ_{odd} extrapolates to somewhat below 100 Hz, reasonably close to the calculated tunneling rate 110 Hz of one quasiparticle on the island.

To model pair breaking caused by backaction, we

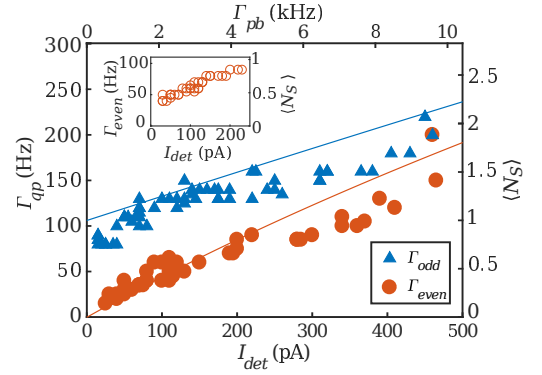


FIG. 4. Quasiparticle tunneling rates Γ_{qp} in sample A corresponding to events out of charge states with even (Γ_{even} , circles) and odd (Γ_{odd} , triangles) parity. Γ_{qp} corresponds to a mean quasiparticle number $\langle N_S \rangle$ according to Eq. (1). The rates decrease with decreasing detector current, and Γ_{even} extrapolates to zero with $I_{det} = 0$. Solid lines are calculated $\langle N_S \rangle$ for $N = 0$ (red) and $N = 1$ (blue) at $n_g = 0.5$ as a function of the Cooper pair breaking rate $\Gamma_{pb} = AI_{det}/e$. Inset: tunneling rates Γ_{even} measured two weeks earlier during the same cooldown extrapolate to 30 Hz at $I_{det} = 0$, which corresponds to $\Gamma_{pb} \approx 1$ kHz.

assume $\Gamma_{pb} = AI_{det}/e$ without a constant detector-independent rate. The fit parameter $A = 1/300,000$ is the probability for an electron tunneling in the detector to break a Cooper pair. We calculate the mean quasiparticle number in even and odd states at $n_g = 0.5$ as a function of Γ_{pb} (Fig. 4) and convert it to a tunneling rate using Eq. (1). Fitting the occupation probabilities and tunneling rates as in Fig. 3 to measurements at different $V_{b,det}$ confirms that the effect of the detector is only to break Cooper pairs, as no other parameters need to be changed for a good fit (data not shown). However, determining the actual backaction mechanism needs further experiments. A similar linear dependence on the current of a nearby SET was observed as quasiparticle poisoning rate measured in a fully superconducting SET in Ref. [9]. The possible processes include shot noise and nonequilibrium phonons generated by quasiparticles recombining in the detector.

The lowest measured Cooper pair breaking rate in sample A is 520 Hz at $V_{b,det} = 390$ μ eV and $I_{det} = 25$ pA, which is to be taken as an upper limit for the background pair breaking rate. We have also observed a reduction of Γ_{pb} extrapolated at $I_{det} = 0$ from 1 kHz to zero during a 3-week cooldown due to unknown reasons (inset of Fig. 4). In sample B, the mean quasiparticle numbers $\langle N_S \rangle$ again decrease with decreasing $V_{b,det}$. By fitting data similar to that shown in Fig. 3, we obtain $\Gamma_{pb} = 100$ Hz at $V_{b,det} = 350$ μ eV, which corresponds to $\langle N_S \rangle = 0.04$ and zero excitations on the island for 97 % of the time. Measuring I_{det} directly is not possible in this setup, but the charge detector of sample B has higher sensitivity at small $V_{b,det}$, allowing smaller detector currents

(estimated $I_{det} < 10$ pA). Therefore, we attribute the decreased $\langle N_S \rangle$ in sample B to reduced detector backaction compared to sample A.

In conclusion, we have observed a clear parity effect in the occupation probabilities and tunneling rates of the charge states of a superconducting island, even in the presence of a single nonequilibrium excitation. The excitations are generated by Cooper pairs breaking on the superconducting island, and they almost always recombine before tunneling out. The poisoning time or parity lifetime of the island—defined as the time between quasiparticle tunneling events—can be long, like in this experiment, even though the island is still poisoned in the sense of quasiparticles being present. The Cooper pair breaking is caused by the backaction of the charge detector, which can be minimized by reducing the detector current. We expect that in future experiments, the statistics of electron counting yields access to the recombination and pair breaking rates independently of each other in a similar manner as in the spin-blockade studies [38–40], where the electron occupation preserving spin flip rate was determined from the tunneling statistics.

This work was performed as part of the Academy of Finland Centre of Excellence program (project 312057). We acknowledge the provision of facilities by Aalto University at OtaNano - Micronova Nanofabrication Centre.

* elsa.mannila@aalto.fi

- [1] M. T. Tuominen, J. M. Hergenrother, T. S. Tighe, and M. Tinkham, *Phys. Rev. Lett.* **69**, 1997 (1992).
- [2] T. M. Eiles, J. M. Martinis, and M. H. Devoret, *Phys. Rev. Lett.* **70**, 1862 (1993).
- [3] P. Lafarge, P. Joyez, D. Esteve, C. Urbina, and M. H. Devoret, *Phys. Rev. Lett.* **70**, 994 (1993).
- [4] P. Lafarge, P. Joyez, D. Esteve, C. Urbina, and M. H. Devoret, *Nature (London)* **365**, 422 (1993).
- [5] J. Aumentado, M. W. Keller, J. M. Martinis, and M. H. Devoret, *Phys. Rev. Lett.* **92**, 066802 (2004).
- [6] S. J. MacLeod, S. Kafanov, and J. P. Pekola, *Appl. Phys. Lett.* **95**, 052503 (2009).
- [7] K. Cedergren, S. Kafanov, J.-L. Smir, J. H. Cole, and T. Duty, *Phys. Rev. B* **92**, 104513 (2015).
- [8] S. Vaitiekėnas, A. M. Whiticar, M. T. Deng, F. Krizek, J. E. Sestoft, S. Marti-Sanchez, J. Arbiol, P. Krogstrup, L. Casparis, and C. M. Marcus, *arXiv:1802.04210*.
- [9] J. Männik and J. E. Lukens, *Phys. Rev. Lett.* **92**, 057004 (2004).
- [10] J. M. Martinis, M. Ansmann, and J. Aumentado, *Phys. Rev. Lett.* **103**, 097002 (2009).
- [11] G. Catelani, J. Koch, L. Frunzio, R. J. Schoelkopf, M. H. Devoret, and L. I. Glazman, *Phys. Rev. Lett.* **106**, 077002 (2011).
- [12] D. Rainis and D. Loss, *Phys. Rev. B* **85**, 174533 (2012).
- [13] A. P. Higginbotham, S. M. Albrecht, G. Kiršanskas, W. Chang, F. Kuemmeth, P. Krogstrup, T. S. Jespersen, J. Nygård, K. Flensberg, and C. M. Marcus, *Nat. Phys.* **11**, 1017 (2015).
- [14] S. M. Albrecht, E. B. Hansen, A. P. Higginbotham, F. Kuemmeth, T. S. Jespersen, J. Nygård, P. Krogstrup, J. Danon, K. Flensberg, and C. M. Marcus, *Phys. Rev. Lett.* **118**, 137701 (2017).
- [15] M. D. Shaw, R. M. Lutchyn, P. Delsing, and P. M. Echternach, *Phys. Rev. B* **78**, 024503 (2008).
- [16] D. Ristè, C. C. Bultink, M. J. Tiggelman, R. N. Schouten, K. W. Lehnert, and L. DiCarlo, *Nat. Commun.* **4**, 1913 (2013).
- [17] P. J. de Visser, J. J. A. Baselmans, P. Diener, S. J. C. Yates, A. Endo, and T. M. Klapwijk, *Phys. Rev. Lett.* **106**, 167004 (2011).
- [18] R. Barends, J. Wenner, M. Lenander, Y. Chen, R. C. Bialczak, J. Kelly, E. Lucero, P. O'Malley, M. Mariantoni, D. Sank, H. Wang, T. C. White, Y. Yin, J. Zhao, A. N. Cleland, J. M. Martinis, and J. J. A. Baselmans, *Appl. Phys. Lett.* **99**, 113507 (2011).
- [19] L. Grünhaupt, N. Maleeva, S. T. Skacel, M. Calvo, F. Levy-Bertrand, A. V. Ustinov, H. Rotzinger, A. Monfardini, G. Catelani, and I. M. Pop, *arXiv:1802.01858*.
- [20] K. J. Stone, K. G. Megerian, P. K. Day, P. M. Echternach, J. Bueno, and N. Llombart, *Appl. Phys. Lett.* **100**, 263509 (2012).
- [21] P. K. Day, H. G. LeDuc, B. A. Mazin, A. Vayonakis, and J. Zmuidzinas, *Nature (London)* **425**, 817 (2003).
- [22] H. S. Knowles, V. F. Maisi, and J. P. Pekola, *Appl. Phys. Lett.* **100**, 262601 (2012).
- [23] V. F. Maisi, S. V. Lotkhov, A. Kemppinen, A. Heimes, J. T. Muhonen, and J. P. Pekola, *Phys. Rev. Lett.* **111**, 147001 (2013).
- [24] D. J. Van Woerkom, A. Geresdi, and L. P. Kouwenhoven, *Nat. Phys.* **11**, 547 (2015).
- [25] M. Lenander, H. Wang, R. C. Bialczak, E. Lucero, M. Mariantoni, M. Neeley, A. D. O'Connell, D. Sank, M. Weides, J. Wenner, T. Yamamoto, Y. Yin, J. Zhao, A. N. Cleland, and J. M. Martinis, *Phys. Rev. B* **84**, 024501 (2011).
- [26] O. Naaman and J. Aumentado, *Phys. Rev. B* **73**, 172504 (2006).
- [27] A. J. Ferguson, N. A. Court, F. E. Hudson, and R. G. Clark, *Phys. Rev. Lett.* **97**, 106603 (2006).
- [28] N. A. Court, A. J. Ferguson, R. Lutchyn, and R. G. Clark, *Phys. Rev. B* **77**, 100501 (2008).
- [29] K. Serniak, M. Hays, G. de Lange, S. Diamond, S. Shankar, L. D. Burkhardt, L. Frunzio, M. Houzet, and M. H. Devoret, *arXiv:1803.00476*.
- [30] D. Aasen, M. Hell, R. V. Mishmash, A. Higginbotham, J. Danon, M. Leijnse, T. S. Jespersen, J. A. Folk, C. M. Marcus, K. Flensberg, and J. Alicea, *Phys. Rev. X* **6**, 031016 (2016).
- [31] T. Karzig, C. Knapp, R. M. Lutchyn, P. Bonderson, M. B. Hastings, C. Nayak, J. Alicea, K. Flensberg, S. Plugge, Y. Oreg, C. M. Marcus, and M. H. Freedman, *Phys. Rev. B* **95**, 235305 (2017).
- [32] O.-P. Saira, A. Kemppinen, V. F. Maisi, and J. P. Pekola, *Phys. Rev. B* **85**, 012504 (2012).
- [33] R. J. Schoelkopf, P. Wahlgren, A. A. Kozhevnikov, P. Delsing, and D. E. Prober, *Science* **280**, 1238 (1998).
- [34] S. Gasparinetti, K. L. Viisanen, O.-P. Saira, T. Faivre, M. Arzeo, M. Meschke, and J. P. Pekola, *Phys. Rev. Appl.* **3**, 014007 (2015).
- [35] K. L. Viisanen, S. Suomela, S. Gasparinetti, O.-P. Saira, J. Ankerhold, and J. P. Pekola, *New J. Phys.* **17**, 055014 (2015).

- [36] J. van Veen, A. Proutski, T. Karzig, D. I. Pikulin, R. M. Lutchyn, J. Nygård, P. Krogstrup, A. Geresdi, L. P. Kouwenhoven, and J. D. Watson, arXiv:1805.10266.
- [37] O. Naaman and J. Aumentado, Phys. Rev. Lett. **96**, 100201 (2006).
- [38] V. F. Maisi, A. Hofmann, M. Rösli, J. Basset, C. Reichl, W. Wegscheider, T. Ihn, and K. Ensslin, Phys. Rev. Lett. **116**, 136803 (2016).
- [39] T. Fujita, P. Stano, G. Allison, K. Morimoto, Y. Sato, M. Larsson, J.-H. Park, A. Ludwig, A. D. Wieck, A. Oiwa, and S. Tarucha, Phys. Rev. Lett. **117**, 206802 (2016).
- [40] K. Ptaszyński, Phys. Rev. B **96**, 035409 (2017).